Surface-emitting terahertz quantum cascade laser source based on intracavity difference-frequency generation

Cite as: Appl. Phys. Lett. **93**, 161110 (2008); https://doi.org/10.1063/1.3009198
Submitted: 29 July 2008 . Accepted: 08 October 2008 . Published Online: 24 October 2008

Christian Pflügl, Mikhail A. Belkin, Qi Jie Wang, Markus Geiser, Alexey Belyanin, Milan Fischer, Andreas Wittmann, Jérôme Faist, and Federico Capasso

Surface-emitting terahertz quantum cascade laser source based on intracavity difference-frequency generation

Christian Pflügl,[1,a)] Mikhail A. Belkin,[1,b)] Qi Jie Wang,[1] Markus Geiser,[1] Alexey Belyanin,[2] Milan Fischer,[3] Andreas Wittmann,[3] Jérôme Faist,[3] and Federico Capasso[1,c)]
[1]*Harvard School of Engineering and Applied Sciences, Harvard University, Cambridge, Massachusetts 02138, USA*
[2]*Department of Physics, Texas A&M University, College Station, Texas 77843, USA*
[3]*Institute of Quantum Electronics, ETH Zürich, CH-8093 Zürich, Switzerland*

(Received 29 July 2008; accepted 8 October 2008; published online 24 October 2008)

We report a surface-emitting terahertz source based on intracavity difference-frequency generation in dual-wavelength midinfrared quantum cascade lasers with integrated giant second-order nonlinear susceptibility. The terahertz light is coupled out of the waveguide by a second-order grating etched into the laser ridges. In contrast to sources where the difference-frequency radiation is extracted from the facet, this approach enables extraction of the terahertz emission from the whole length of the device even when the coherence length is small. © *2008 American Institute of Physics*. [DOI: 10.1063/1.3009198]

Intracavity nonlinear light generation in quantum cascade lasers (QCLs) (Refs. 1 and 2) has attracted considerable attention over the past several years. Recent developments led to the realization of a new electrically pumped semiconductor terahertz source working at room temperature (RT).[3] The source is based on intracavity difference-frequency generation (DFG) in dual-wavelength midinfrared (mid-IR) QCLs with giant optical nonlinearity monolithically integrated in the active region.[4] Generating terahertz radiation via intracavity DFG in mid-IR QCLs circumvents the problems that are limiting the high temperature operation of conventional terahertz QCLs.[5,6] Since mid-IR QCLs have been shown to operate continuous wave (cw) with more than 1.5 W of output power at RT (Ref. 7) and the optical nonlinearity for DFG does not significantly deteriorate with temperature,[3] this approach can lead to an electrically pumped cw RT semiconductor terahertz source with optical power in the milliwatt range, which would be of practical interest in applications.

DFG is a nonlinear optical process in which two beams at frequencies ω_1 and ω_2 interact in a medium with second-order nonlinear susceptibility, $\chi^{(2)}$, to produce radiation at frequency $\omega=\omega_1-\omega_2$. For collinear interaction, the power of the wave at frequency $\omega=\omega_1-\omega_2$ is given by the expression[2,4,8]

$$W(\omega=\omega_1-\omega_2)=\frac{\omega^2}{8\varepsilon_0 c^3 n(\omega_1)n(\omega_2)n(\omega)}|\chi^{(2)}|^2\frac{W(\omega_1)W(\omega_2)}{S_{\text{eff}}}l_{\text{coh}}^2, \quad (1)$$

where $l_{\text{coh}}=1/[(k_1-k_2-k)^2+(\alpha/2)^2]$ is the coherence length, $W(\omega_i)$, $n(\omega_i)$, and k_i are the power, refractive index, and the real wave vector of the beam at frequency $\omega_i(i=1,2)$, respectively, α stands for the losses at the DFG frequency, and S_{eff} is the effective area of interaction (see Refs. 2 and 4).

The coherence length in terahertz QCL sources based on intracavity DFG is typically limited to hundreds of microns by the free-carrier absorption at terahertz frequencies.[3,4] On the other hand, a typical QCL waveguide is 2–5 mm long. Thus, most of the terahertz light generated via intracavity DFG in the device is lost due to the free-carrier absorption. This problem can be avoided if terahertz radiation is extracted vertically from the whole length of the waveguide using the surface-emission scheme. In this case the terahertz power is proportional to the top emitting area of the device, L_xL_y; see Fig. 1(a). Furthermore, the large emitting area in surface-emitting devices would result in a more directional terahertz output, in comparison with the edge-emitting devices. Surface-emitting distributed feedback (DFB) lasers with second-order grating have been demonstrated for regular mid-IR and far-IR QCLs[9–13] and for intracavity second-harmonic generation in QCLs.[14] In this letter we report on surface-emitting terahertz QCL sources based on intracavity DFG.

The surface emission in our terahertz sources is achieved using a second-order grating for the terahertz wave. We note, however, that there is an important difference between our surface-emitting terahertz sources and the surface-emitting DFB QCLs with second-order gratings demonstrated previously.[9–14] The second-order gratings implemented for standard QCLs[9–13] matched the wave vector of a given laser mode, whereas in our devices the grating should match the wave vector of the nonlinear polarization at difference frequency; see below. Furthermore, for devices reported in Refs. 9–13 the gratings strongly affected lasing conditions by introducing additional losses and DFB. Second-order gratings in QCLs with intracavity second-harmonic generation also acted simultaneously as a DFB cavity for the laser mode at the fundamental frequency.[14] This resulted in single-mode emission for these devices. In the case of the devices reported in this work, a second-order grating for terahertz DFG wave can only act as a very-high-order DFB grating for the mid-IR modes (approximately 12th-order and 10th-order gratings for the mid-IR pumps in our case). In addition, the spatial extension of the terahertz mode is much larger than

a)Electronic mail: pflugl@seas.harvard.edu.
b)Present address: Department of Electrical and Computer Engineering, University of Texas at Austin, Austin, TX 78758. Electronic mail: mbelkin@ece.utexas.edu.
c)Electronic mail: capasso@seas.harvard.edu.

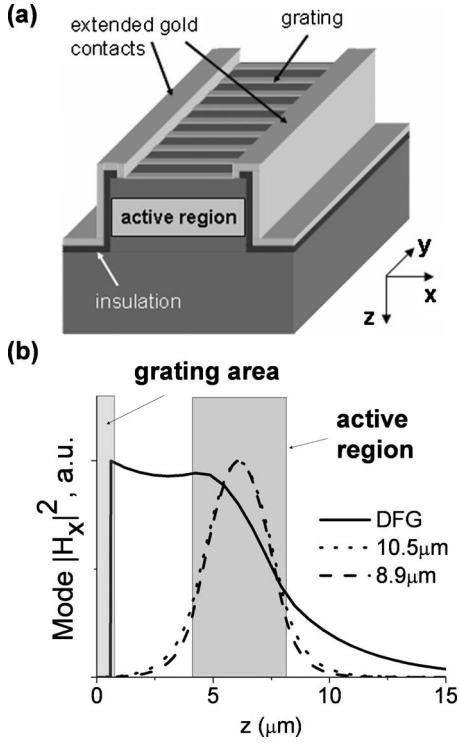

FIG. 1. (a) Schematic drawing of the ridge waveguide structure with the gold grating on top. (b) The TM_{00} mode profiles for the terahertz wave ($\lambda \approx 60\ \mu m$) generated via DFG and the two mid-IR pumps ($\lambda_1 \approx 8.9\ \mu m$ and $\lambda_2 \approx 10.5\ \mu m$). The mode profiles were calculated for the waveguide without grating that consists of a 400 nm thick layer of gold, a 200 nm thick InP plasmon layer (n doped $5\times10^{18}\ cm^{-3}$), a 3.5 μm thick InP cladding layer (n doped $5\times10^{16}\ cm^{-3}$), a 6 μm thick active region, and an InP substrate (n doped $1\times10^{17}\ cm^{-3}$). The position of the active region and depth of the grating grooves (~300 nm) are indicated in gray. The grating is etched through the top plasmon layer and 100 nm into the lower doped top InP cladding layer.

that of mid-IR modes and the second-order grating for terahertz emission in our device has little interaction with the mid-IR laser modes [see Fig. 1(b)]. Thus, the grating coupling strength to the mid-IR modes is poor and, as a result, multimode mid-IR and terahertz emission spectra are expected for our devices.

The terahertz radiation in our devices is generated by the nonlinear polarization $P^{(2)}$ induced by the two mid-IR pumps in the QCL active region with nonlinear susceptibility, $\chi^{(2)}$.[3,4,8] We can express $P^{(2)}$ as

$$P^{(2)}(x,y,z,t) = \varepsilon_0 \chi^{(2)}(x,z) \times E^z_{\omega_1}(x,z) E^z_{\omega_2}(x,z) e^{-i[(\omega_1-\omega_2)t-(k_1-k_2)y]}, \quad (2)$$

where the z-direction [see Fig. 1(a)] is perpendicular to the waveguide layers, the y-direction is along the waveguide, and $E^z_{\omega_1}(x,z)$ and $E^z_{\omega_2}(x,z)$ are the z-components of the electric field amplitudes of the two mid-IR waves at frequencies ω_1 and ω_2, respectively. The propagation wave vector for a terahertz mode $H(x,y,z,t)$ in a QCL waveguide generated by $P^{(2)}$ equals to that of $P^{(2)}$, see Refs. 4 and 8,

$$H(x,y,z,t) \sim \frac{\varepsilon_0 \omega}{2} \frac{e^{-i[(\omega_1-\omega_2)t-(k_1-k_2)y]}}{i[k-(k_1-k_2)]+\alpha/2}. \quad (3)$$

For efficient diffraction outcoupling of the terahertz mode in a QCL waveguide into the radiation emitted from the surface, the grating wave vector must be chosen to match the wave vector of the terahertz wave in a QCL waveguide. In the case of our devices, effective modal indices for the mid-IR laser modes at wavelengths $\lambda_1 \approx 8.9\ \mu m$ and $\lambda_2 \approx 10.5\ \mu m$ were calculated using COMSOL and were found to be equal to ≈3.19 and ≈3.176, respectively. This corresponds to $k_1 - k_2 \approx 3515\ cm^{-1}$ and the grating period $2\pi/k_g \approx 17.9\ \mu m$, which was chosen to be the grating period of the reported devices. We note that grating-outcoupled surface emission can be generated even in the absence of any guided in-plane terahertz modes. In this case the nonlinear polarization is directly coupled to electromagnetic modes radiated from the surface. In the case of our devices, the diffraction outcoupling of the terahertz waveguide mode is likely to dominate the surface emission because our devices are designed to support a terahertz waveguide mode and have very long coherence length on the order of 50–80 μm for intracavity terahertz DFG.[3]

A slight mismatch between the grating wave vector and that of the terahertz wave in a QCL waveguide will result in a surface-emission wave propagating at a slight angle to the grating surface normal with a nonzero horizontal wave vector component $k_y = k_1 - k_2 - k_g$. The output power should be only weakly dependent on the mismatch. The diffraction efficiency and therefore the output power, however, are sensitive to the waveguide and grating geometry. We are currently performing systematic studies of the diffraction efficiency for different device geometries and the results will be published elsewhere.

The active region and waveguide structure of a QCL material used in this work are identical to that reported in Ref. 3. The active region is comprised of a two-stack InGaAs/InAlAs active region, lattice matched to InP, with integrated giant optical nonlinearity for the DFG process. A detailed discussion on the bandstructure design and the performance of the edge-emitting ridge lasers fabricated for this material can be found in Ref. 3. The devices discussed in this work were processed into surface-emitting ridge waveguide lasers with a grating on top of the ridges. The processing started with reactive ion etching (RIE) of the 28 μm wide ridges using a silicon nitride mask deposited via chemical vapor deposition. After that, a 300 nm thick silicon nitride insulation layer was deposited conformally and opened on top of the ridge. The metal (Ti/Au, 5 nm/200 nm)/air grating was defined by lift-off on top of the ridges to form the structures shown in Fig. 1(a). Finally, 300 nm of the top waveguide cladding was removed in the grating openings via RIE, using the metal grating as a mask. The current in our devices is injected through the sides of the ridge; see Fig. 1(a).[9] After the processing, the wafers were thinned to approximately 250 μm and cleaved into approximately 1 mm long laser bars. The laser bars were indium mounted on copper heatsinks and the lasers were wire bonded. Finally, a high-reflection coating (Al_2O_3/Ti/Au) was deposited on the back facets of the devices to improve their performance.

For the measurements, our devices were operated in pulsed mode with 60 ns pulses at a 250 kHz repetition rate. Terahertz radiation was collected using two 2 in. diameter parabolic mirrors: one with a 5 cm focal length to collect light from the device and the other with a 15 cm focal length to refocus it onto a He-cooled calibrated silicon bolometer. The output power for the mid-IR beams was measured using a calibrated thermopile detector. Spectra were taken with a

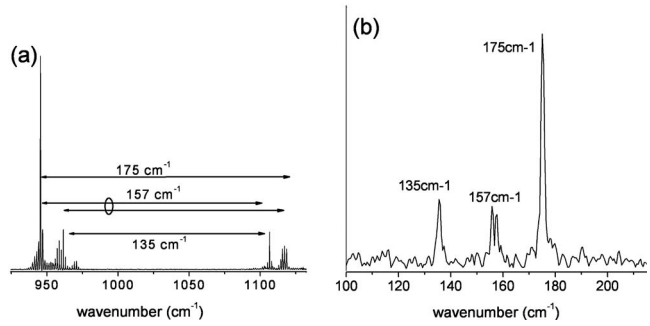

FIG. 2. (a) The mid-IR emission spectrum collected from the edge of a typical device operated in pulsed mode at 80 K. (b) The terahertz emission spectrum from the surface of the device in (a).

Fourier transform IR spectrometer. For terahertz measurements, mid-IR radiation was blocked using optical filters.

Figure 2 shows the mid-IR and terahertz spectra of a typical device, taken at 80 K. The positions of the peaks in the terahertz spectrum correspond to the frequency difference between the peaks in the mid-IR spectrum. Figure 3 shows the *LI* characteristics for the mid-IR and terahertz light at 80 K. The maximum mid-IR power output of a 1 mm long device at 80 K was measured to be 3.5 W. The maximum terahertz output power via the surface was measured to be ~1 μW (corrected for approximately ~10% collection efficiency of our terahertz setup). The detected output power via the uncoated facet was a factor of 4 lower. We measured several devices and found the ratio for surface to facet emission to be in the range of 2–5. The total power however varied significantly, which can be led back to the appearance of higher order modes observed for the 8.9 μm pump beam. The terahertz intensity decreased with decreasing power of the mid-IR pump beams. Both mid-IR modes were still observed at RT with a combined power of about 700 mW. The DFG signal (~70 nW) however was too weak for spectral

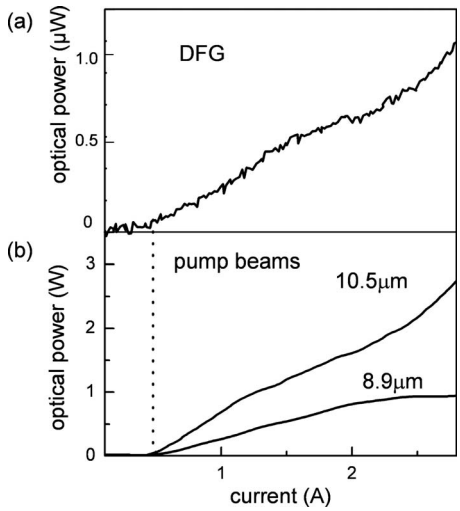

FIG. 3. The *LI* characteristics of the device of Fig. 2 for (a) the terahertz signal and (b) the two mid-IR pump beams measured in pulsed mode at 80 K.

characterization. At the present stage, these devices have lower terahertz output power than normal ridge lasers with a silicon hyperhemispherical lens attached to the device facet reported in Ref. 3. The use of gratings, however, is potentially more promising as it allows extracting the terahertz radiation from the whole length of the device.

In future work we plan to improve the waveguide design to enhance the surface-emission efficiency and perform a systematic experimental study of the influence of the grating period and other grating parameters such as duty cycle and groove depth on the surface-emission efficiency. Eventually, circular structures, with top gratings for the terahertz light, can improve both the output power and beam quality. These structures would have very low outcoupling losses for the mid-IR pump beams, resulting in low threshold current densities and high pump intensity. Additionally, these structures are expected to provide a very low divergence terahertz output.[15]

This work was supported by USAFOSR under Contract No. FA9550–05–1–0435. A.B. acknowledges support from NSF through Grant No. ECS-0547019 (CAREER). Sample growth was partly done at the University of Neuchatel. The structures were processed at the Center for Nanoscale Science in Harvard University, which is a member of the National Nanotechnology Infrastructure Network. The authors would like to acknowledge the help of Nicolas Hoyler.

[1]N. Owschimikow, C. Gmachl, A. Belyanin, V. Kocharovsky, D. L. Sivco, R. Colombelli, F. Capasso, and A. Y. Cho, Phys. Rev. Lett. **90**, 043902 (2003).
[2]C. Gmachl, A. Belyanin, D. L. Sivco, M. L. Peabody, N. Owschimikow, A. M. Sergent, F. Capasso, and A. Y. Cho, IEEE J. Quantum Electron. **39**, 1345 (2003).
[3]M. A. Belkin, F. Capasso, F. Xie, A. Belyanin, M. Fischer, A. Wittmann, and J. Faist, Appl. Phys. Lett. **92**, 201101 (2008).
[4]M. A. Belkin, F. Capasso, A. Belyanin, D. L. Sivco, A. Y. Cho, D. C. Oakley, C. J. Vineis, and G. W. Turner, Nat. Photonics **1**, 288 (2007), and supplementary information.
[5]B. S. Williams, Nat. Photonics **1**, 517 (2007).
[6]M. A. Belkin, J. A. Fan, S. Hormoz, F. Capasso, S. P. Khanna, M. Lachab, A. G. Davies, and E. H. Linfield, Opt. Express **16**, 3242 (2008).
[7]A. Lyakh, C. Pflügl, L. Diehl, Q. J. Wang, F. Capasso, X. J. Wang, J. Y. Fan, T. Tanbun-Ek, R. Maulini, A. Tsekoun, R. Go, and C. K. N. Patel, Appl. Phys. Lett. **92**, 111110 (2008).
[8]Y. R. Shen, *The Principles of Nonlinear Optics* (Wiley, New York, 1984).
[9]D. Hofstetter, J. Faist, M. Beck, and U. Oesterle, Appl. Phys. Lett. **75**, 3769 (1999).
[10]C. Pflügl, M. Austerer, W. Schrenk, S. Golka, G. Strasser, R. P. Green, L. R. Wilson, J. W. Cockburn, A. B. Krysa, and J. S. Roberts, Appl. Phys. Lett. **86**, 211102 (2005).
[11]O. Demichel, L. Mahler, T. Losco, C. Mauro, R. Green, J. H. Xu, A. Tredicucci, F. Beltram, H. E. Beere, D. A. Richie, and V. Tamosiunas, Opt. Express **14**, 5335 (2006).
[12]J. A. Fan, M. A. Belkin, F. Capasso, S. Khanna, M. Lachab, A. G. Davies, and E. H. Linfield, Opt. Express **14**, 11672 (2006).
[13]S. Kumar, B. S. Williams, Q. Qin, A. W. M. Lee, Q. Hu, and J. Reno, Opt. Express **15**, 113 (2007).
[14]M. Austerer, C. Pflügl, S. Golka, W. Schrenk, A. M. Andrews, T. Roch, and G. Strasser, Appl. Phys. Lett. **88**, 121104 (2006).
[15]L. Mahler, A. Tredicucci, R. P. Green, F. Beltram, C. Walther, and J. Faist, Proceedings of the CLEO, 2008 (unpublished).